The influence of impurities on soliton dynamics in stacked systems

1990 J. Phys.: Condens. Matter 2 4081

(http://iopscience.iop.org/0953-8984/2/18/005)

J. Phys.: Condens. Matter **2** (1990) 4081–4097. Printed in the UK

The influence of impurities on soliton dynamics in stacked systems

Detlef Hofmann, Wolfgang Förner, Peter Otto and Janos Ladik
Friedrich-Alexander-Universität Erlangen-Nürnberg, D-8520 Erlangen, Egerlandstrasse 3, Federal Republic of Germany

Received 14 March 1989, in final form 18 December 1989

Abstract. By numerical simulation of the classical equations of motion the soliton dynamics in stacked systems containing formamide and thioformamide units were studied. Each unit in the stack has three geometrical degrees of freedom. The existence of solitary waves in both systems and their transmission, absorption and reflection at impurities were numerically studied.

As has been pointed out by Ladik [1], simple statistical considerations show that the probability of removing a blocking protein from DNA only by local effects is too small to explain carcinogenesis. Therefore different possibilities for the activation of oncogenes by long-range effects caused by carcinogens have been discussed [2]. One of these invokes the concept of solitary waves [3]. Solitons are localised excitations rather than wave packets of large amplitudes. They propagate without change in shape or loss of energy and thus survive collisions with other solitons. Solitons arise in non-linear and dispersive systems [4]. Solitary waves are soliton-like excitations which do not exactly fulfil the soliton conditions. There are two distinct groups of solitons defined. One group contains the topological solitons, where the potential has two (e.g. in the ϕ^4 theory) or more degenerate ground states. In this case the soliton is the domain wall between two regions of the system which are in different ground states. For the second group, the non-topological or conformational solitons only one ground state exists. Here the soliton is a localised, mostly travelling distortion of this ground state which is stabilised by the non-linear forces in the system.

The soliton concept is also used to explain other phenomena in physics and chemistry. The 'ϕ^4-potential' *ansatz* was applied to describe soliton dynamics in the sugar-phosphate backbone of DNA [5] and phase transitions, i.e. in $Pb_5Ge_3O_{11}$ [6]. The 'sine–Gordon' equation is applied to ferromagnetic [7] and antiferromagnetic [8] materials and to the dynamics of rotations around carbon–carbon bonds in polyethylene [9]. The charge transport in lightly doped *trans*-polyacetylene can be related to topological solitons via a Hückel-type [10, 11] or Pariser–Parr–Pople (PPP) Hamiltonian [12–14]. A soliton mechanism is also proposed for the storage and transport of energy in proteins [15, 16].

In a first test for the hypothesis of a soliton mechanism in the case of chemical carcinogenesis a stacked arrangement of formamide molecules was numerically studied

0953-8984/90/184081 + 17 $03.50

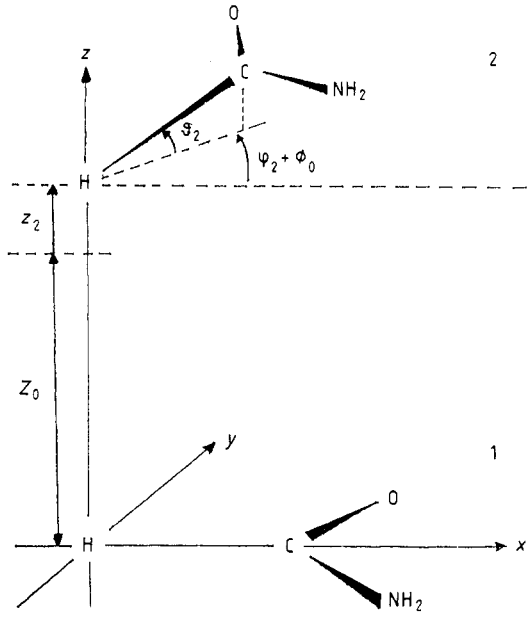

Figure 1. Geometry of a formamide dimer and definition of the geometrical variables.

[17]. In this case, only conformational solitons are possible. These calculations followed the formalism given by Ladik and Čížek [3], which is based on the Su–Schrieffer–Heeger (SSH) Hamiltonian [10]. For this purpose the SSH theory had to be generalised to three geometrical degrees of freedom for each nucleotide base [3]. Using the definition for the geometrical variables as given by Krumhansel and Alexander [5], z_n was defined as the shift of the nth unit out of its equilibrium position in the direction of the helix axis, φ_n describes the rotation of a base around this axis and ϑ_n measures the tilting relative to this axis (see figure 1). To get a structure similar to B-DNA [18] an equilibrium distance of 3.36 Å was chosen and for the rotation between two consecutive molecules $\phi_0 = 36°$. In real DNA, Z_0 and ϕ_0 are independent of the sequence of bases in the stack but they depend on the conformation of the given DNA helix (e.g. A-, B-, C- or Z-DNA). However, in our model system, Z_0 and ϕ_0 can be adjusted with the help of the linear backbone potential to any desired value (see below). Thus we have chosen $Z_0 = 3.36$ Å and $\phi_0 = 36°$ as in B-DNA. To analyse the influence of aperiodicity, thioformamide was introduced as a perturbation into the chain. Thioformamide represents a much larger aperiodicity in a formamide stack than the different nucleotide bases in DNA; however, in this case the effects of perturbation are more marked. As has been discussed in [19] the masses of the solitons are expected to be large enough to neglect the quantum effects in the equations of motion. This allows the use of classical equations of motion. In a comparison of PPP [20–23] with Hückel-type models as well as with classical potential calculations, no significant differences were found [24]. This justifies a classical *ansatz* for the potential surface. For that reason the potential is written as

$$E = E_{BB} + E_{VI}. \tag{1}$$

E_{VI} (where VI stands for 'vertical interaction') is given as a sum of pair potentials between next neighbours. E_{BB} simulates the backbone, which stabilises the stack in the

equilibrium geometry. As discussed below, we use for E_{BB} in this model study the simplest possible *ansatz*, i.e. the only information contained in E_{BB} in our model is that it should stabilise the otherwise repulsive stack in the predefined equilibrium geometry. This term will be replaced by exact calculations on the DNA backbone in the future. E_{VI} has been expanded into a Taylor series of sixth order as a function of the variables at sites n and $n+1$ ($\{\Delta z_n\}$, $\{\Delta\vartheta_n\}$ and $\{\Delta\varphi_n\}$) taking into account the types of molecule at these sites (denoted by t_n and t_{n+1}, respectively). Δz_n is defined as

$$\Delta z_n = z_{n+1} - z_n \tag{2}$$

and analogously for $\Delta\vartheta_n$ and $\Delta\varphi_n$. Thus E_{VI} can be written as

$$E_{VI} = \sum_{n=1}^{N-1} \sum_{i,j,k\geq 0}^{i+j+k\leq 6} C_{ijkt_{n+1}t_n} (\Delta z_n)^i (\Delta\vartheta_n)^j (\Delta\varphi_n)^k. \tag{3}$$

For E_{BB} a linear *ansatz* is used:

$$E_{BB} = \sum_{n=1}^{N-1} (A_{zt_n}\Delta z_n + A_{\vartheta t_n}\Delta\vartheta_n + A_{\varphi t_n}\Delta\varphi_n). \tag{4}$$

The requirement that the equilibrium geometry (denoted by the subscript eq) represents the minimum of the total potential energy leads to

$$(\partial E/\partial z_n)|_{eq} = 0 \tag{5}$$

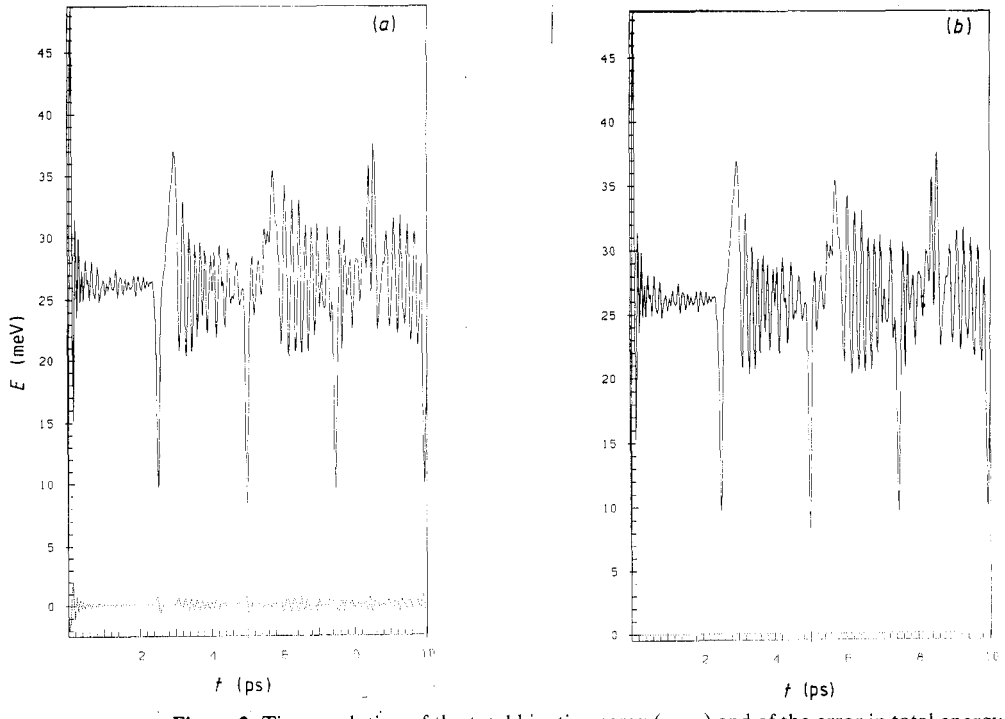

Figure 2. Time evolution of the total kinetic energy (——) and of the error in total energy (– – –) for the collision of two solitary waves (see caption for figure 4(*a*) for details) using (*a*) a one-step procedure and (*b*) a fourth-order Runge–Kutta method.

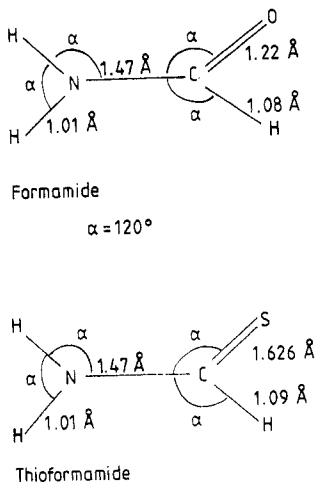

Figure 3. Geometry of formamide and thioformamide molecules as used in the calculations of potential surfaces.

and finally together with (4) to

$$A_{zt_n} = -(\partial E_{\mathrm{VI}}/\partial z_n)|_{\mathrm{eq}} = C_{100t_{n+1}t_n} - C_{100t_nt_{n-1}}. \tag{6}$$

Therefore A_{zt_n} is only equal to zero if all three molecules at sites $n-1$, n and $n+1$ are of the same kind. Thus A_{zt_n} is clearly a redundant parameter since it only shifts the linear part of the Taylor series to zero in the equilibrium geometry. In this way, condition (5) is fulfilled and the predefined equilibrium geometry represents the potential minimum if $(\partial^2 E/\partial z_n^2)_{\mathrm{eq}} > 0$ holds, which is the case in our model system. Otherwise a more complicated *ansatz* for E_{BB} has to be introduced. Of course, for ϑ_n and φ_n, similar considerations hold.

The discrete form of the equations of motion was used:

$$\begin{aligned} M_n \ddot{z}_n(i) &= F_{z_n}(i) & F_{z_n}(i) &= -\partial E(i, z_n, \vartheta_n, \varphi_n)/\partial z_n \\ \theta_{\vartheta_n} \ddot{\vartheta}_n(i) &= F_{\vartheta_n}(i) & F_{\vartheta_n}(i) &= -\partial E(i, z_n, \vartheta_n, \varphi_n)/\partial \vartheta_n \\ \theta_{\varphi_n} \ddot{\varphi}_n(i) &= F_{\varphi_n}(i) & F_{\varphi_n}(i) &= -\partial E(i, z_n, \vartheta_n, \varphi_n)/\partial \varphi_n \end{aligned} \tag{7a}$$

Table 1. Type of potential surface (F stands for formamide and T for thioformamide), the number (N) of points calculated on it, the largest error $E_{\max}$ and the average error E_{av} of the sixth-order fit for E_{VI}.

Type	N	$E_{\max}$ (mHartree)	E_{av} (mHartree)
F–F[a]	701	0.434	0.053
T–F	601	0.644	0.071
F–T	601	1.225	0.135
T–T	601	1.291	0.214

[a] A–B stands for a dimer where B follows A in the helix direction.

Table 2. The ten largest accelerations I (in nano atomic units) in a formamide (FF) and a thioformamide (TT) dimer for two geometrical distortions (absolute values given) together with the corresponding order of the term in the Taylor expansion of the potential surface (i for Δz, j for $\Delta\vartheta$ and k for $\Delta\varphi$; $I = (\partial E/\partial z)/M$ in all cases except the two indicated by [a]) where $I = (\partial E/\partial\vartheta)/\theta_\vartheta$; geometry A is given by $\Delta z = 0.5$ Å, $\Delta\vartheta = \Delta\varphi = 15°$ and geometry B by $\Delta z = 0.25$ Å. $\Delta\vartheta = \Delta\varphi = 7.5°$).

FF, A				TT, A				FF, B				TT, B			
i	j	k	I	i	j	k	I	i	j	k	I	i	j	k	I
3	1	0	55.614	2	1	0	143.866	2	0	0	13.351	2	0	0	44.599
3	2	0	52.143	3	1	0	133.250	1	1	0	9.677	1	1	0	38.156
4	1	0	41.775	2	2	0	120.390	2	1	0	9.656	2	1	0	35.966
2	2	0	41.128	3	2	0	96.828	3	0	0	7.660	3	0	0	20.562
2	1	0	38.625	2	0	0	89.199	3	1	0	6.951	3	1	0	16.656
3	1	1	31.736	3	0	0	82.250	2	2	0	5.141	1	2	0	16.173
3	0	0	30.643	4	1	0	82.181	4	0	0	3.802	2	2	0	15.048
4	0	0	30.419	1	1	0	76.312	1	2	0	3.655	0	2	0	13.141[a]
4	1	1	29.881	1	2	0	64.693	3	2	0	3.258	1	0	1	8.666
2	3	0	29.763	4	0	0	63.621	0	2	0	2.952[a]	4	0	0	7.952

and

$$\begin{aligned}\dot{z}_n(i+1) &= \dot{z}_n(i) + \tau_0 F_{z_n}(i)/M_n \\ \dot{\vartheta}_n(i+1) &= \dot{\vartheta}_n(i) + \tau_0 F_{\vartheta_n}(i)/\theta_{\vartheta_n} \\ \dot{\varphi}_n(i+1) &= \dot{\varphi}_n(i) + \tau_0 F_{\varphi_n}(i)/\theta_{\varphi_n}\end{aligned} \tag{7b}$$

where i indicates the time step under consideration. Note that the equations are coupled through the dependence of E on all geometrical degrees of freedom. For the integration the forces $F_n(i)$ are assumed to be constant over a time step τ_0 ($\tau_0 = 0.006$ ps in all computations). The second integration following Su and Schrieffer [11] leads to

$$\begin{aligned}z_n(i+1) &= z_n(i) + \tau_0 \dot{z}_n(i+1) \\ \vartheta_n(i+1) &= \vartheta_n(i) + \tau_0 \dot{\vartheta}_n(i+1) \\ \varphi_n(i+1) &= \varphi_n(i) + \tau_0 \dot{\varphi}_n(i+1).\end{aligned} \tag{8}$$

Since this integration scheme appears to be rather crude we have computed the dynamics shown in figure 4(a) (see below) also with the help of a fourth-order Runge–Kutta method using the same τ_0. The time evolution of the local kinetic energy shown in figure 4(a) (see below) is the same for both methods without any visible difference. In figure 2 we show the time evolution of the total kinetic energy (full curve) and of the error in total energy (broken curve), as obtained with both methods. Obviously the total kinetic energy is the same in both cases. Only the error in the total energy shows some negligible oscillations around zero in the case of the one-step procedure. Therefore we used the less time-consuming one-step method as described above.

In figure 3 the exact geometry of the calculated constituent molecules is shown. The four different types of coefficients c_{ijk} have been determined by a least-squares fit to *ab initio* Hartree–Fock potential surfaces. The surfaces have been computed with the help of the GAUSSIAN 74 program [25]. For our model study a minimal atomic basis set has been applied (STO-3G [25]). The number of points calculated on the potential surfaces

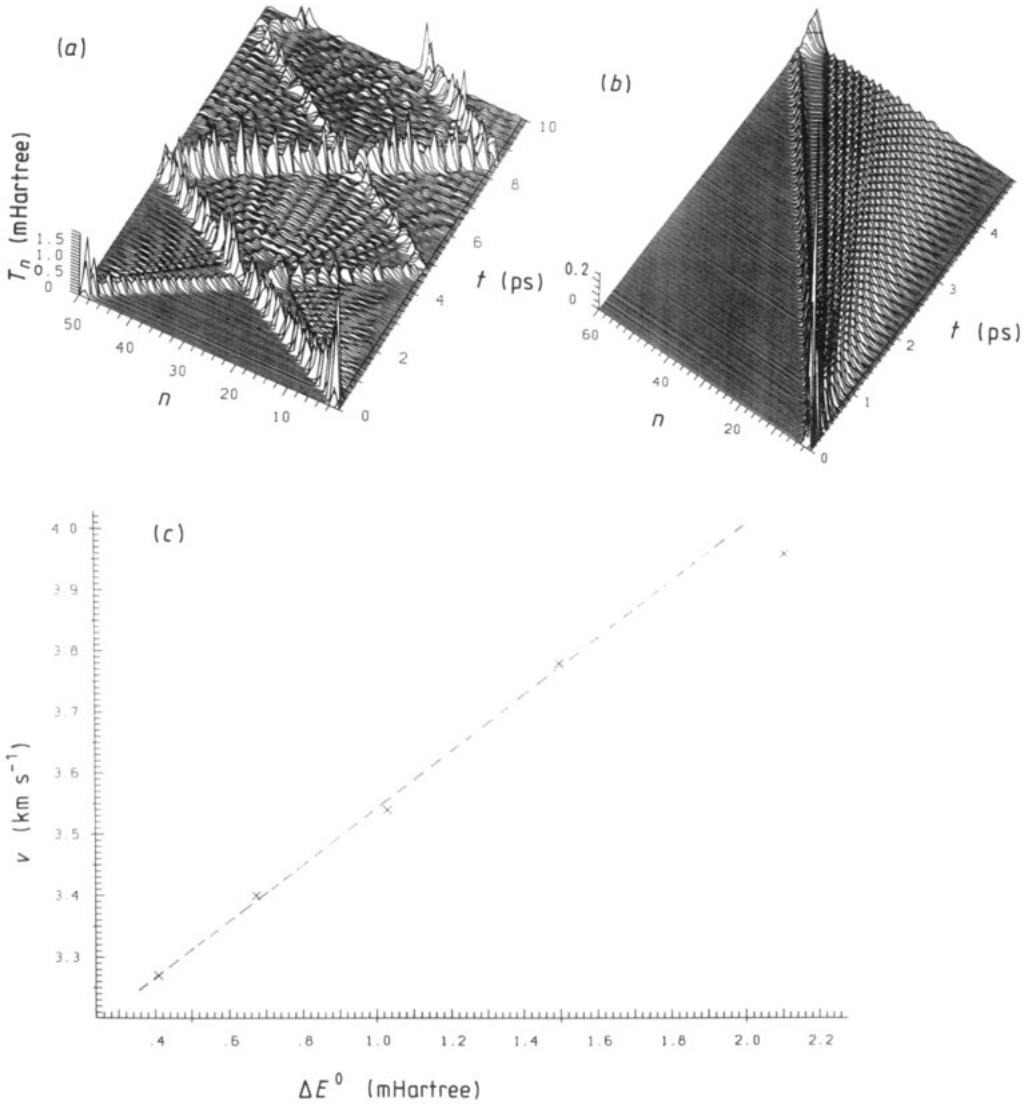

Figure 4. Propagation of solitary waves: local kinetic energy T_n as a function of site n and time t. (*a*) Collision of two different solitary waves in a formamide stack with initial elongation $z_2 = -0.8$ Bohr, $z_{49} = 0.6$ Bohr. (*b*) Propagation of a solitary wave in a thioformamide stack with, initial elongation $z_2 = -0.4$ Bohr. (*c*) Soliton velocity as a function of initial excitation energy ΔE^0 in polyformamide.

and the average errors of the least-squares fits are listed in table 1. The maximal errors seem to be quite large compared with the total kinetic energy of the examined solitary waves (see below), but these are not due to the order of the Taylor series. They occur because the dimers for the calculation of the surfaces were chosen to depend on four variables (ϑ_1, ϑ_2, φ_2 and z_2). In order to be able to describe the interaction energy as a function of three variables we calculated $\Delta\vartheta = \vartheta_2 - \vartheta_1$ which is only valid for small ϑ. The range of ϑ (and φ) was from $-15°$ up to $+15°$. Therefore the large maximal errors occur at the limits of the fitting region and are larger than those previously reported [17].

However, the distortions occurring in our simulations are much smaller than these limits.

To decide which coefficients in the potential are the most important, we show in table 2 the ten largest accelerations in formamide and thioformamide dimers for two distortions from the equilibrium geometry. Obviously for the large distortion the most important Taylor coefficients belong to fourth and fifth order, while for the smaller distortion the second and third orders appear to be most important. This shows that the higher orders of the series are most important at the borders of the fitting region, while for moderate distortions (as used in the simulations shown below) they appear to be unimportant. However, one has to keep in mind that, in more realistic DNA models, larger distortions have to be treated than here. Therefore the potential surface of nucleotide base stacks has to be computed to a higher accuracy than for our formamide stacks. It is, however, obvious from our model study that for an accurate fit of potential surfaces of this kind Taylor series up to sixth order are necessary (see also [19]).

The results of our dynamical simulations are displayed graphically. Namely the local kinetic energy T_n given by

$$T_n = \tfrac{1}{2}(M_n \dot{z}_n^2 + \theta_{\vartheta_n} \dot{\vartheta}_n^2 + \theta_{\varphi_n} \dot{\varphi}_n^2) \tag{9}$$

is shown as function of site n and time. M_n is the mass; θ_{ϑ_n} and θ_{φ_n} are the moments of inertia of the molecule at site n. T_n is given in mHartree. During our dynamic simulations the conservation of energy, total momentum and the two components of total angular momentum is examined to exclude numerical errors.

In figure 4, solitary waves in the pure systems (polyformamide and polythioformamide) are shown. In figure 4(a) site 2 is elongated to -0.8 Bohr, and site 49 to $+0.6$ Bohr. The two other geometrical variables ϑ and φ and all other molecules are kept in their equilibrium positions. In figure 4(b) the second molecule is elongated by -0.4 Bohr. The properties of solitary waves (passing through one another; long lifetime) can be recognised for polyformamide very well. The velocity of the waves in polyformamide is about 3.6 km s^{-1} while in polythioformamide it is about 5 km s^{-1}.

The dependence of the velocity of the solitary waves on their excitation energy is approximately linear for excitation energies less than about 2 mHartree, as can be seen from figure 4(c) for formamide. However, the slope of the linear part in figure 4(c) is very small. This agrees with our findings on chains with open ends [19] where, probably because of the more qualitative measurement of the velocities there, the soliton velocity is independent of the excitation energy or the kinetic energy transported. Thus, for the solitons considered, we found a strong dependence of their kinetic mass on the excitation energy. We could not observe solitons at rest under any initial condition considered. We cannot detect a possible proportionality of ΔE^0 to v^2 for $v \to 0$ since for $v \to 0$ very small excitation energies would be necessary. In this case, solitons most probably would not exist or would be impossible to detect. Until now we have not been able to find linear excitations similar to wave packets using the potential surfaces computed for formamide and thioformamide. However, if the potential terms of orders larger than two are neglected the usual dispersive wave packet solutions have been found numerically [19].

In figure 5 the influence of an isolated perturbation is shown. In figure 5(a) the time evolution of the local kinetic energy is shown from the same perspective as in figure 4(a). However, to be able to obtain also quantitative information about the loss of energy of the soliton due to impurities the perspective used in figure 5(b) is preferable. In order to present full information about our results (also off the soliton world line) we show both perspectives for most of the examples. In figures 5(a) and 5(b), site 20 of polythioformamide is replaced by one formamide molecule, and in figures 5(c) and 5(d) the two

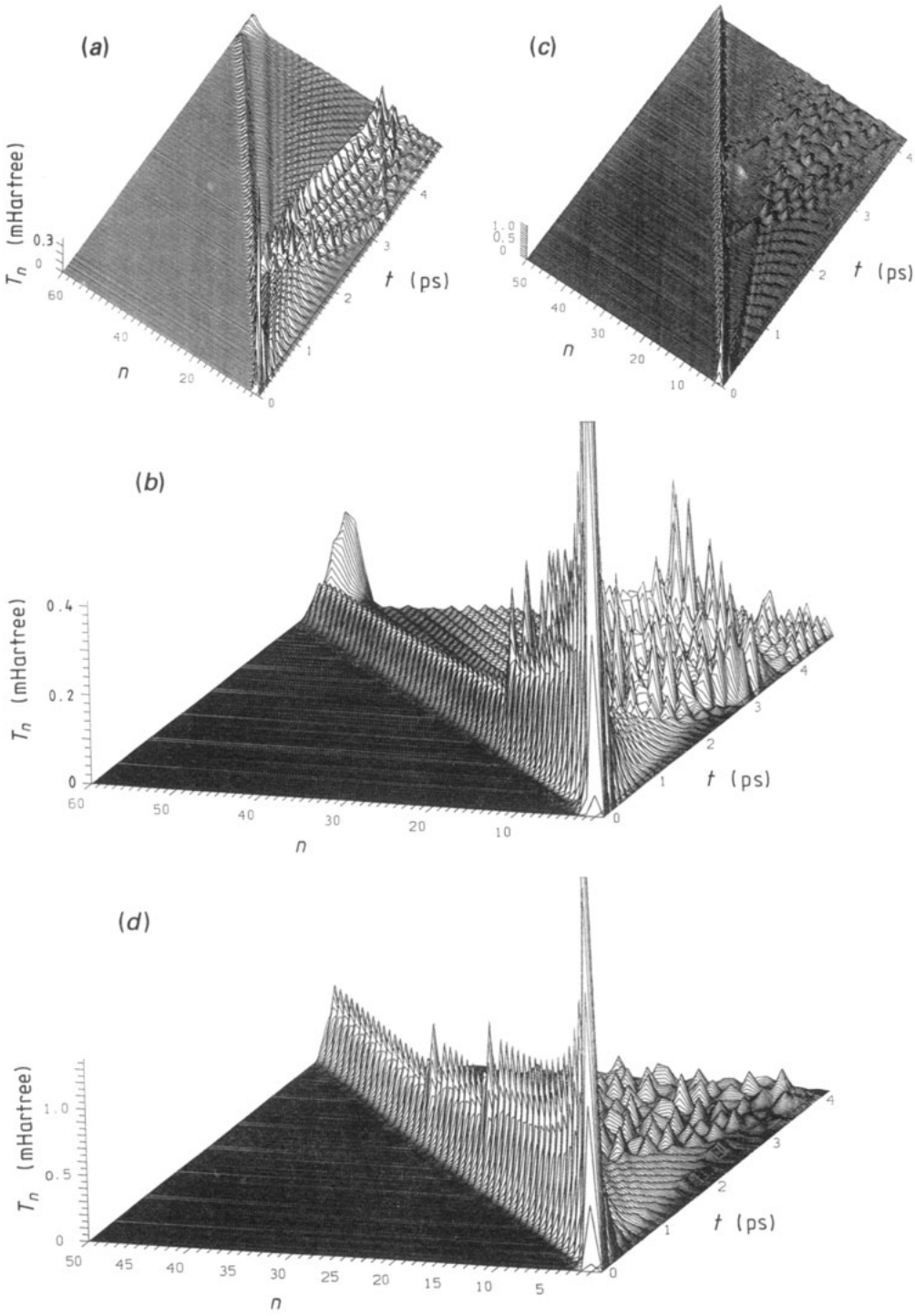

Figure 5. Influence of isolated impurities on solitary waves. (*a*) Formamide (site 20) in polythioformamide with initial elongation $z_2 = -0.4$ Bohr. (*b*) Same as (*a*) but from another perspective. (*c*) Thioformamide (sites 20 and 30) in polyformamide with initial elongation $z_2 = -0.8$ Bohr. (*d*) Same as (*c*) but from another perspective.

sites 20 and 30 of polyformamide by thioformamide. The initial elongation of site 2 is, in figures 5(*a*) and 5(*b*), −0.4 Bohr and in figures 5(*c*) and 5(*d*), −0.8 Bohr. At the impurities a fraction of the energy of the solitary wave is reflected and another fraction absorbed in both cases (thioformamide in polyformamide and vice versa). A transmission coefficient can be deduced. From figure 5 the height of the kinetic energy peak before and after a collision with the perturbation can be measured. The resulting transmission coefficient is about 0.5 in the first case (formamide in polythioformamide) and about 0.75 in the second case (thioformamide in polyformamide).

A thioformamide impurity in a formamide stack acts in two ways. First of all it has a larger mass and larger moments of inertia, and secondly its interaction with the neighbouring molecules is stronger than the formamide–formamide interaction. The latter is due to the larger spatial extension of the sulphur p_z atomic orbital in comparison with the oxygen orbitals.

In figure 6(*a*) the maximum T_m of the local kinetic energy is plotted as a function of time for polyformamide after an initial excitation of $z_2 = -0.8$ Bohr in a chain of 60 units. After a short relaxation the oscillations are perfectly periodic up to the first reflection at roughly 5 ps. After reflection the oscillations become disturbed since the soliton moves now in an already distorted chain. In figure 6(*b*) the local kinetic energy T_n is shown as a function of site n after 2.78 ps. It is obvious that the soliton is very narrow (roughly 3 units) and most of the kinetic energy is localised at one single unit. Thus the 58 oscillations seen in figure 6(*a*) can be interpreted as the transfer of the kinetic energy from one unit to the next.

In figure 6(*c*), T_n is shown after 2.82 ps in a chain where at unit 18 a thioformamide molecule is present. Obviously the passing of the impurity changes the height but not the shape of the energy packet. A part of the kinetic energy is scattered back at the impurity and the velocity of the soliton is somewhat reduced. Figure 6(*d*) shows T_n in the chain without an impurity after 4.64 ps. Obviously the energy packet does not change shape or height with time (compare with figure 6(*b*)). This is confirmed by figure 6(*e*) where T_n is shown after two reflections at the chain ends (11.9 ps). The width and shape of the peak in the kinetic energy corresponding to the soliton is independent of the initial excitation. We have checked this numerically by computations using $z_2 = -0.8$ Bohr, −0.6 Bohr, −0.4 Bohr and −0.2 Bohr as the initial excitation. Only the height of the peak decreases with decreasing z_2, while its width and shape are unchanged. However, for $z_2 = -0.2$ Bohr the peak height is already smaller than the disturbances behind it. Thus for this excitation it is not clear whether a real soliton or a dispersive wave packet is formed.

In the coordinate space the soliton gives rise to a rather complicated structure in all three geometrical variables. This can be seen in figures 6(*f*)–6(*h*) (z_n, ϑ_n and φ_n as functions of site n after 2.78 ps). The energy of the soliton is localised in the steep descent of z_n, ϑ_n and φ_n between sites 31 and 35. The distortion relaxes very slowly with a low kinetic energy. Therefore the distorted region of the chain broadens with time as can be seen from figure 6(*i*) (z_n after 4.64 ps). However, the energy is still localised in the steep descent on the right-hand side. A clearly defined soliton coordinate cannot be deduced from figure 6.

In figure 7(*a*) we show for comparison the case of a thioformamide impurity in a formamide stack at unit 20. In figure 7(*b*), only mass and moments of inertia at site 20 have been changed to the thioformamide values while, in figure 7(*c*), for these quantities the formamide values have been used but for the interaction between units 20 and 21, and units 19 and 20, respectively, the formamide–thioformamide potential was applied.

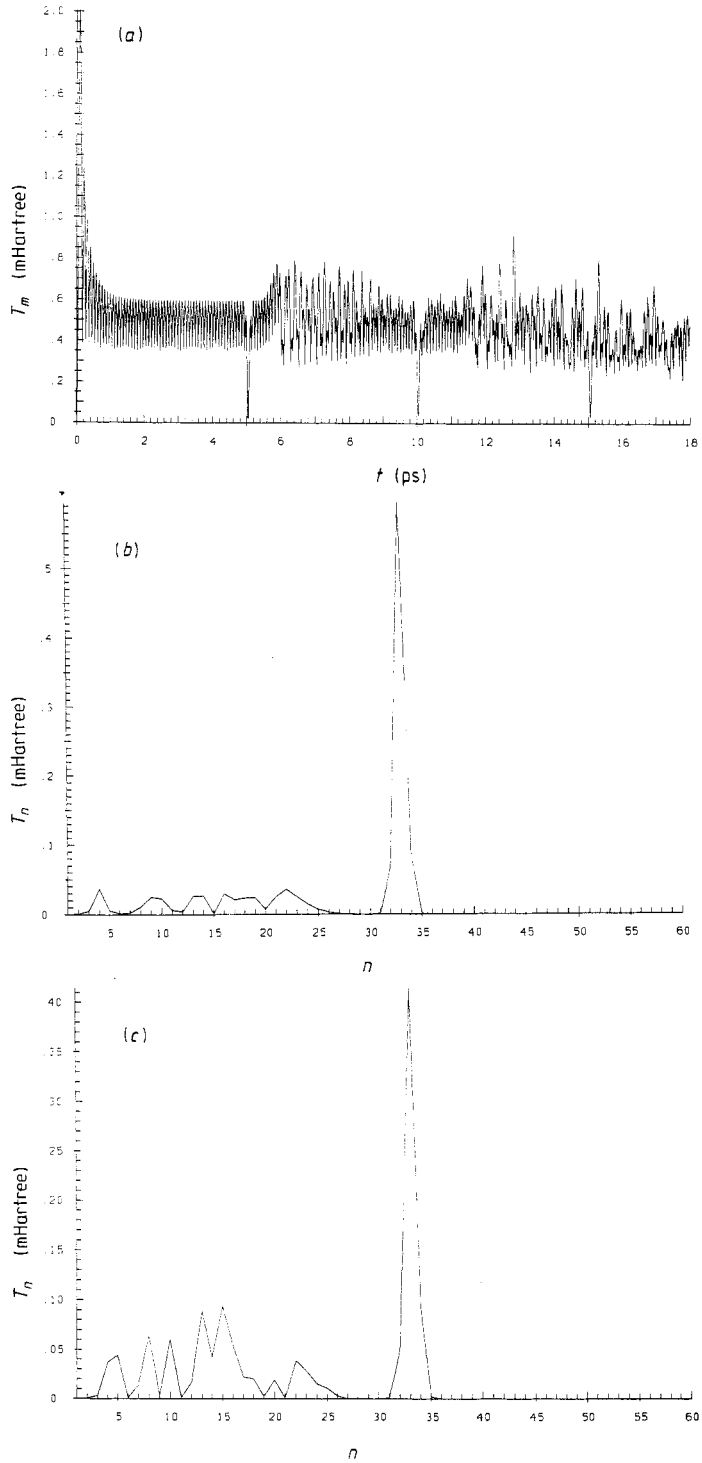

Figure 6. Soliton properties in a chain of 60 formamide units after an initial elongation of $z_2 = -0.8$ Bohr. (*a*) Maximum T_m of the local kinetic energy as a function of time t. (*b*) Local kinetic energy T_n as function of site n after 2.78 ps. (*c*) Same as (*b*) after 2.82 ps in a chain with one thioformamide molecule at site 18. (*d*) Same as (*b*) after 4.64 ps. (*e*) Same as (*b*) after two reflections (11.9 ps). (*f*) z_n as function of site n after 2.78 ps. (*g*) ϑ_n as function of site n after 2.78 ps. (*h*) φ_n as function of site n after 2.78 ps. (*i*) z_n as a function of site n after 4.64 ps.

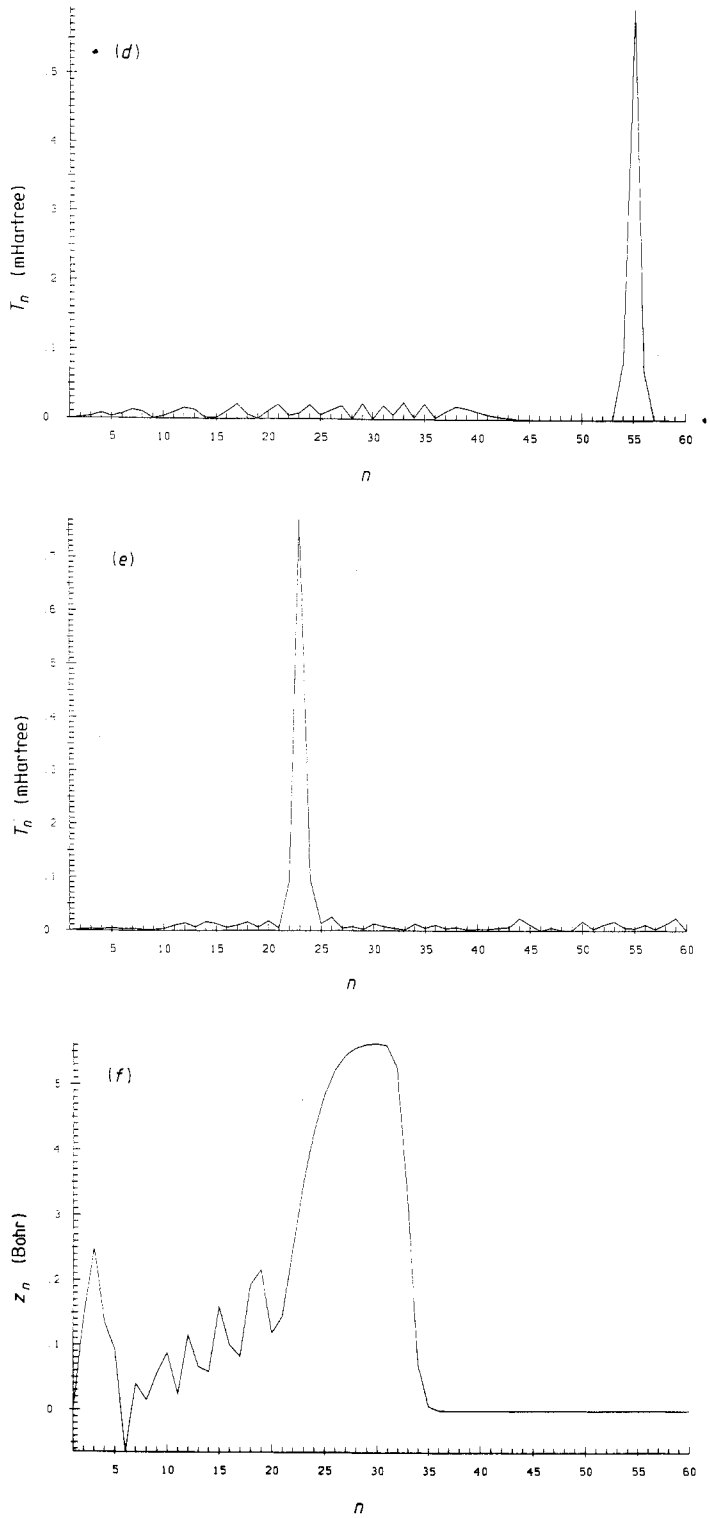

Figure 6 (*continued*)

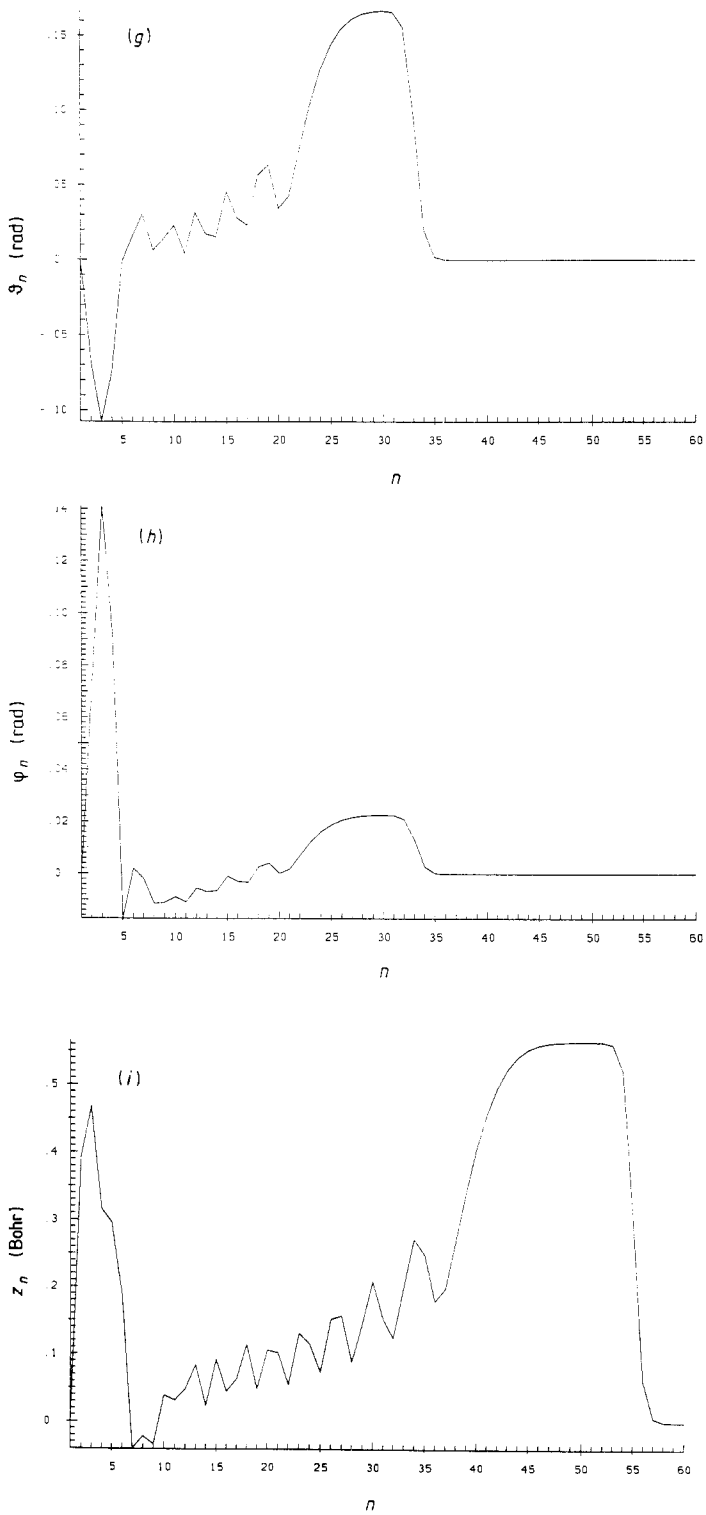

Figure 6 (*continued*)

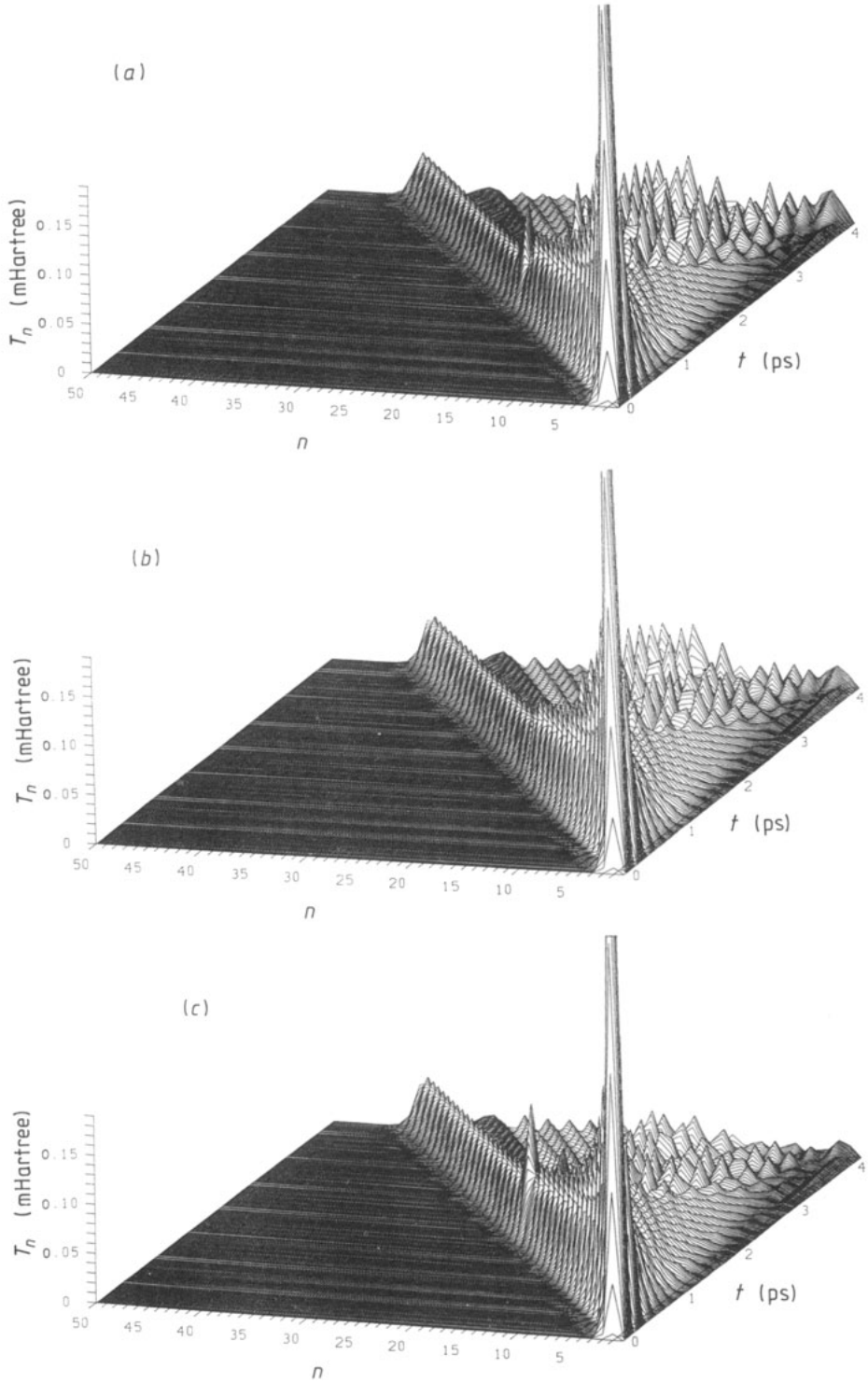

Figure 7. Influence of changes in mass, momenta of inertia and interaction energies due to an impurity on solitary waves in polyformamide with an initial elongation $z_2 = -0.4$ Bohr. (*a*) Site 20 is replaced by thioformamide. (*b*) Site 20 has the mass and momenta of inertia of thioformamide, but the interaction energy between formamide molecules. (*c*) Site 20 has the interaction energy between formamide (sites 19 and 21) and thioformamide, but the mass and moments of inertia as formamide.

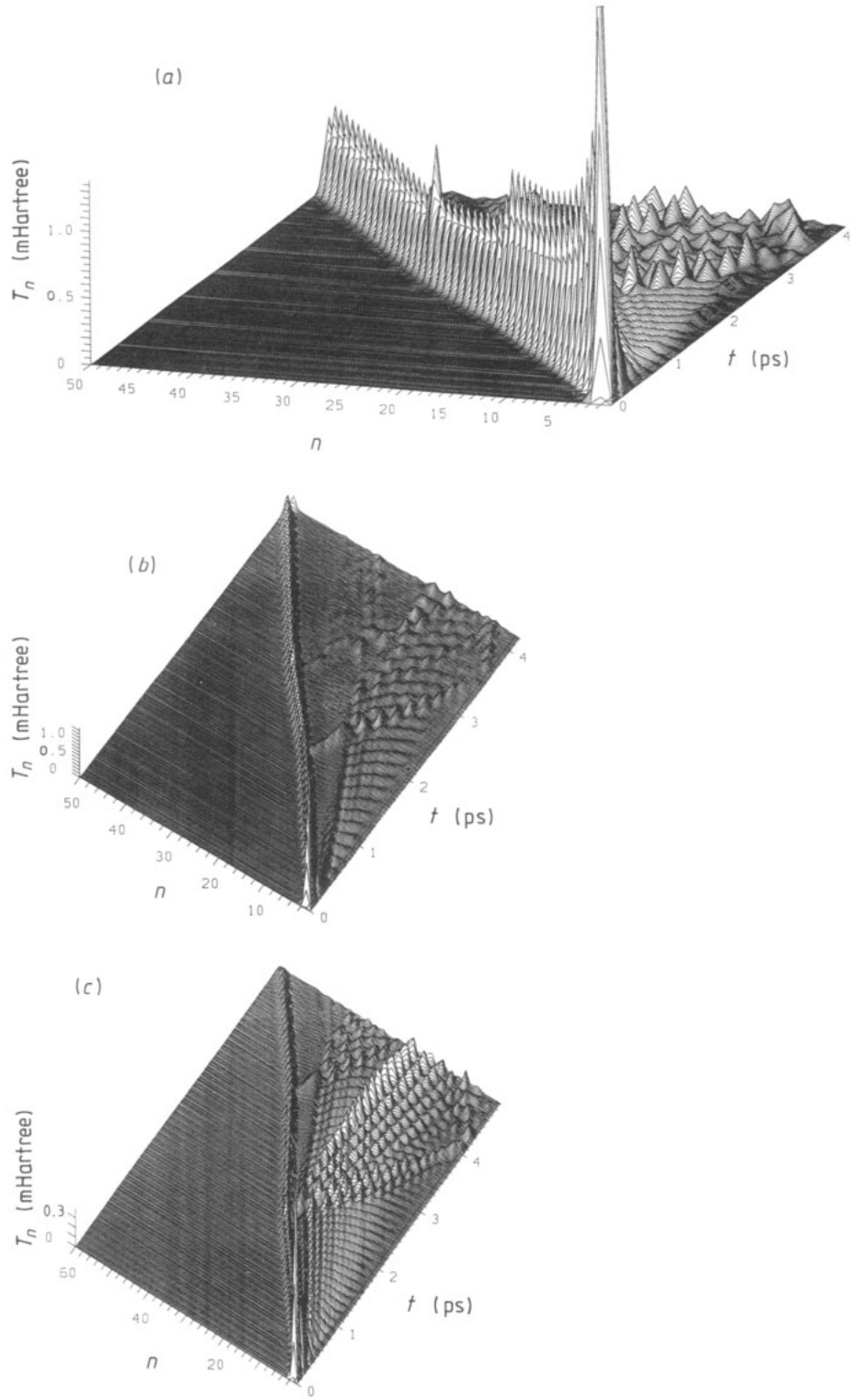

Figure 8. Influence of cumulated impurities. (*a*) Thioformamide (at sites 20–30) in a formamide stack with initial elongation $z_2 = -0.8$ Bohr. (*b*) Same as (*a*) but from another perspective. (*c*) Formamide (at sites 25–40) in a thioformamide stack with initial elongation $z_2 = -0.4$ Bohr.

Obviously the decrease in energy of the solitary wave results from both mass and potential variation in equal amounts. Thus a perturbation acts on solitary waves both through its different mass and moments of inertia and through its different interaction potential.

In figure 8, at sites 20–30, 11 thioformamide molecules are embedded in a formamide stack. The different velocity of the wave in the thioformamide segment is clearly visible. In figure 8(*b*) the same simulation is shown from a different point of view. The similarity of this picture to the transmission of light through media of different optical densities is striking. Reflection and absorption at the boundaries between the two 'media' as well as transmission with different velocities for 'media' of different 'optical densities' are clearly visible.

In figure 9, thioformamide molecules are randomly distributed in a formamide stack. The figure shows that the total effect on the solitary wave can be explained from the observations described above for isolated or cumulated impurities. The effects of the impurities are completely additive. Since this effect should hold also for a second pass of the soliton through the chain or for longer chains with more impurities, one can conclude that the loss of soliton energy will be an exponential function of the number of impurities passed. However, thioformamide represents a rather large impurity in polyformamide. In real DNA for example, one has to deal with the base pairs adenine–thymine (AT) and guanine–cytosine (GC) which differ much less from each other than do formamide and thioformamide both in interactions and in masses. Thus in aperiodic DNA we expect a much larger soliton lifetime than in our model system with large impurities. For instance the ratio of masses of GC to AT is 1.004, while that of thioformamide to formamide is roughly 1.4.

The calculations suggest that each aperiodicity diminishes the energy of a solitary wave. The extent might be proportional to the difference (e.g. mass or interaction energy) between the molecules of the chain and the impurity. The small soliton width is obviously the reason for both the strong effect of impurities and the additivity of the effects of isolated impurities. The dependence of our results on the soliton width cannot be studied within this model system since the width is a property of the system investigated and there are no adjustable parameters in the mathematical model. Our model (although three dimensional) bears some similarity to the Toda [26] lattice, which consists of a linear chain of particles bound by a potential which contains an exponential and a linear term.

Studies of impurity effects have been performed, e.g. for the SSH [27] and the SSH-PPP [28] Hamiltonians, for Davydov solitons [29] and also for other cases (see references [27–29]). In these cases, however, aperiodicity can be introduced just by changing parameters, i.e. no potential surface calculations are necessary. In the case of the Toda lattice, which bears some similarity to our model, we are not aware of any study of impurity effects. Li *et al* [30] studied the influence of one or two impurities in non-linear lattices with either a cubic and quartic or a Morse potential between nearest neighbours. They introduced impurities by changing only the particle mass at one or two sites. They show numerically that for small energies the linear scattering approximation is valid but breaks down for larger energies. They discuss the fact that solitons are more robust than linear wave packets and they find strong interference effects in the case of two impurities. To obtain information about the existence of solitons in DNA it will be necessary to examine the influence of the hydrogen-bonded second strand. Also it will be necessary to replace the backbone potential by a more realistic one. This can be done by introducing additional terms in the potential. Work along these lines is in progress in our laboratory.

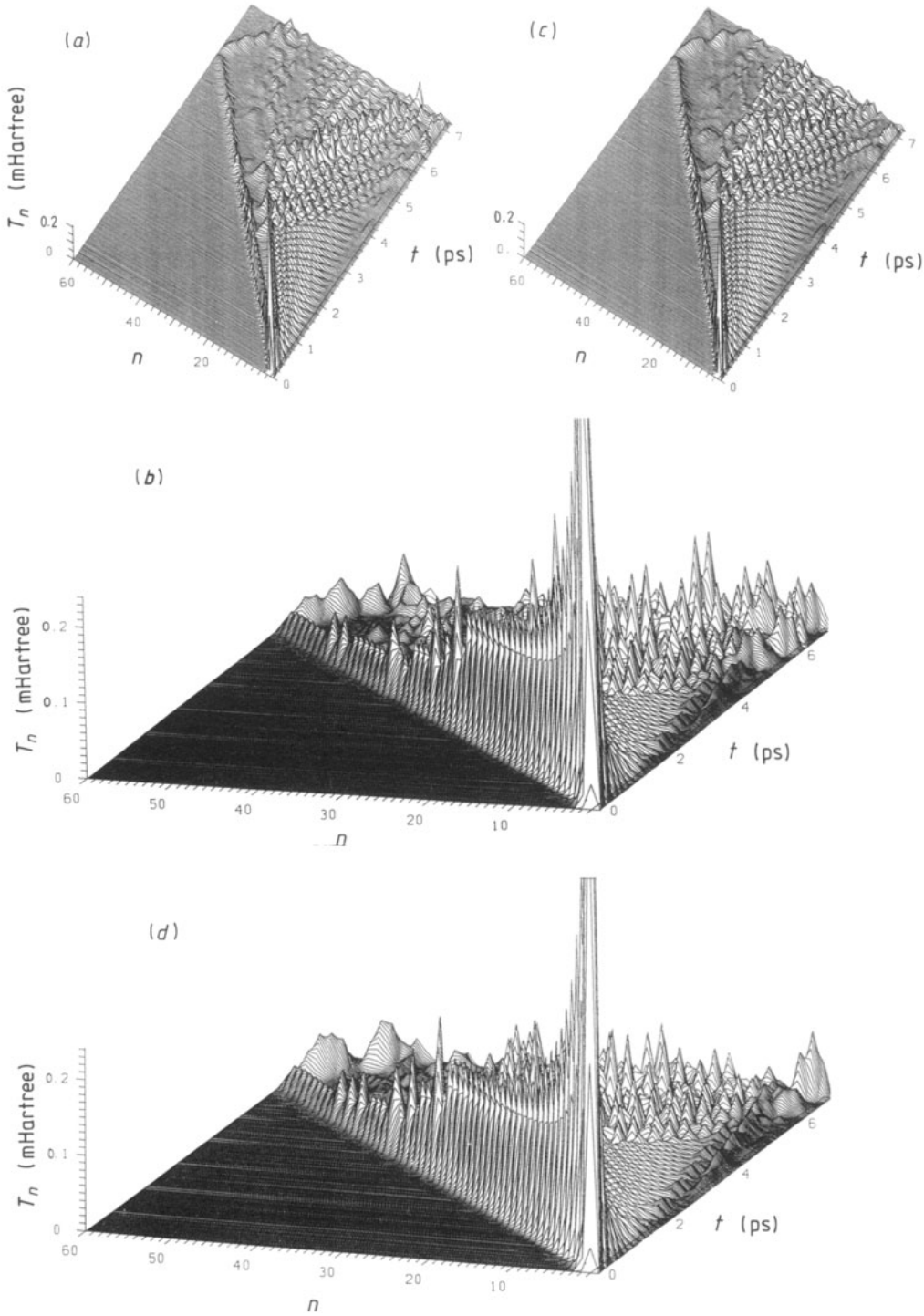

Figure 9. Influence of randomly distributed thioformamide molecules in a formamide stack with initial elongation $z_2 = -0.5$ Bohr. (*a*) Thioformamide at sites 27, 31, 37–39, 48 and 50. (*b*) Same as (*a*) but from another perspective. (*c*) Thioformamide at sites 31, 36, 38, 39, 45, 47 and 49. (*d*) Same as (*c*) but from another perspective.

In the case of DNA, however, in addition environmental effects are of importance, which are also under study. However, the present study indicates that solitary waves exist also in aperiodic stacked systems with a very large difference of the constituent molecules.

Acknowledgments

The financial support of the Fonds der Chemischen Industrie and of the Deutsche Forschungsgemeinschaft (Project Ot 51/6-1) are gratefully acknowledged.

References

[1] Ladik J 1986 *Int. J. Quant. Chem.* **QBS-13** 307
[2] Ladik J, Suhai S and Seel M 1978 *Int. J. Quant. Chem.* **QBS-5** 35
[3] Ladik J and Čížek J 1984 *Int. J. Quant. Chem.* **26** 955
[4] Collins M A 1983 *Adv. Chem. Phys.* **53** 225
[5] Krumhansl J A and Alexander D M 1983 *Structure and Dynamics: Nucleic Acid and Proteins* ed E Clementi and R H Sarma (New York: Adenine Press) p 61
[6] Collins M A, Blumen A, Currie J F and Ross J 1979 *Phys. Rev.* B **19** 3630
[7] Mikeska H J 1978 *J. Phys. C: Solid State Phys.* **11** L29
[8] Maki K 1980 *J. Low. Temp. Phys.* **41** 327
[9] Wahlstrand K J 1985 *J. Chem. Phys.* **82** 5247
Wahlstrand K J and Woylnes P G 1985 *J. Chem. Phys.* **82** 5259
[10] Su W P, Schrieffer J R and Heeger A J 1980 *Phys. Rev.* B **22** 2099
[11] Su W P and Schrieffer J R 1980 *Proc. Natl Acad. Sci. USA* **77** 5626
[12] Wang C L and Martino F 1986 *Phys. Rev.* B **34** 5540
[13] Förner W 1987 *Solid State Commun.* **63** 941
[14] Förner W, Wang C L, Martino F and Ladik J 1988 *Phys. Rev.* B **37** 4567
[15] Davydov A S 1979 *Phys. Scr.* **20** 387
[16] Davydov A S 1982 *Usp. Fiz. Nauk* **138** 603; 1982 *Sov. Phys.–Usp.* **25** 898
[17] Hofmann D, Förner W and Ladik J 1988 *Phys. Rev.* A **37** 4429
[18] Arnott S, Dover S D and Wonacott A J 1969 *Acta Crystallogr.* B **25** 2192
[19] Förner W 1988 *Phys. Rev.* A **38** 939
[20] Pariser R and Parr R G 1953 *J. Chem. Phys.* **21** 466, 707
[21] Pople J A 1953 *Trans. Faraday Soc.* **49** 1375
[22] Ladik J 1965 *Acta Phys. Acad. Sci. Hung.* **18** 185
[23] Ladik J, Rai D K and Appel K 1968 *J. Mol. Spectrosc.* **27** 72
[24] Förner W, Ladik J, Otto P and Martino F 1990 *Phys. Rev.* A at press
[25] Pople J A and Hehre W 1974 GAUSSIAN 74, *Quantum Chemistry Program Exchange (QCPE) Program No 236* (Indiana University)
[26] Toda M 1967 *J. Phys. Soc. Japan* **22** 431; **23** 501
[27] Förner W, Seel M and Ladik J 1986 *Solid State Commun.* **57** 463; 1986 *J. Chem. Phys.* **84** 5910
Phillpot S R, Baeriswyl D, Bishop A R and Lomdahl P S 1987 *Phys. Rev.* B **35** 7533
[28] Markus R, Förner W and Ladik J 1988 *Solid State Commun.* **68** 135
[29] Motschmann H, Förner W and Ladik J 1989 *J. Phys.: Condens. Matter* **1** 5083
Förner W and Ladik J 1990 *Self Trapping of Vibrational Energy in Proteins, Proc. NATO–MIDIT Workshop on Davydov Solitons (1989)* ed P L Christiansen and A C Scott (New York: Plenum) at press
[30] Li Q, Pnevmatikos St, Economou E N and Soukoulis C M 1988 *Phys. Rev.* B **37** 3534